Received: 25 May 2020 | Revised: 9 July 2020 | Accepted: 19 July 2020

DOI: 10.1111/cbdd.13768

RESEARCH ARTICLE

WILEY

Novel phenolic antimicrobials enhanced activity of iminodiacetate prodrugs against biofilm and planktonic bacteria

Danica J. Walsh[1,2] | **Tom Livinghouse**[1] | **Greg M. Durling**[1] | **Adrienne D. Arnold**[2,3] | **Whitney Brasier**[2] | **Luke Berry**[1] | **Darla M. Goeres**[2] | **Philip S. Stewart**[2]

[1]Chemistry and Biochemistry, Montana State University, Bozeman, MT, USA

[2]Center for Biofilm Engineering, Montana State University, Bozeman, MT, USA

[3]Microbiology and Immunology, Montana State University, Bozeman, MT, USA

Correspondence
Tom Livinghouse, Chemistry and Biochemistry, Montana State University, Bozeman, MT, 59717, USA.
Email: livinghouse@montana.edu

Funding information
National Institute for General Medical Science, Grant/Award Number: GM 116949

Abstract

Prodrugs are pharmacologically attenuated derivatives of drugs that undergo bioconversion into the active compound once reaching the targeted site, thereby maximizing their efficiency. This strategy has been implemented in pharmaceuticals to overcome obstacles related to absorption, distribution, and metabolism, as well as with intracellular dyes to ensure concentration within cells. In this study, we provide the first examples of a prodrug strategy that can be applied to simple phenolic antimicrobials to increase their potency against mature biofilms. The addition of (acetoxy)methyl iminodiacetate groups increases the otherwise modest potency of simple phenols. Biofilm-forming bacteria exhibit a heightened tolerance toward antimicrobial agents, thereby accentuating the need for new antibiotics as well as those, which incorporate novel delivery strategies to enhance activity toward biofilms.

KEYWORDS

antimicrobial, anti-biofilm, drug-conjugate, pro-drugs

1 | INTRODUCTION

The majority of bacteria naturally reside in accumulations called biofilms, which exhibit a substantially increased tolerance toward antimicrobials compared to free-floating cells (Hall & Mah, 2017; Venkatesan, Perumal, & Doble, 2015). A biofilm is a community of bacteria that have adhered to a surface, either biotic or abiotic. Once attached, cells begin to secrete extracellular polymeric substances (EPS) composed of extracellular DNA, polysaccharides, and proteins. The EPS traps nutrients and water within the biofilm, allowing cells to mature under nutrient rich conditions while being protected from desiccation, host immune defenses, and antimicrobial agents (Costerton, Stewart, & Greenberg, 1999; Flemming & Wingender, 2010; Malheiro & Simões, 2017; Walters, Roe, Bugnicourt, Franklin, & Stewart, 2003). As a consequence of these defense mechanisms, biofilms are associated with three out of four microbial infections in the body and are responsible for around 1.7 million hospital-acquired infections per year (Khatoon, McTiernan, Suuronen, Mah, & Alarcon, 2018), resulting in nearly 100 thousand deaths annually in the United States (Bryers, 2008).

One factor leading to the resilience of biofilm-mediated infections can be retarded penetration of charged antimicrobial agents due to binding by the robust EPS matrix, thereby hindering complete access throughout the biofilm (Campanac, Pineau, Payard, Baziard-Mouysset, & Roques, 2002; Davenport, Call, & Beyenal, 2014; Donlan & Costerton, 2002; Flemming et al., 2016; Stewart, 2015). Another more important obstacle in treating biofilms is the dormancy of cells within the interior, due to low levels of nutrients and oxygen. This reduced activity cell state is less susceptible to conventional antibiotics, which work best on actively dividing cells (Conlon et al., 2013; Stewart, 2002). The inability of common

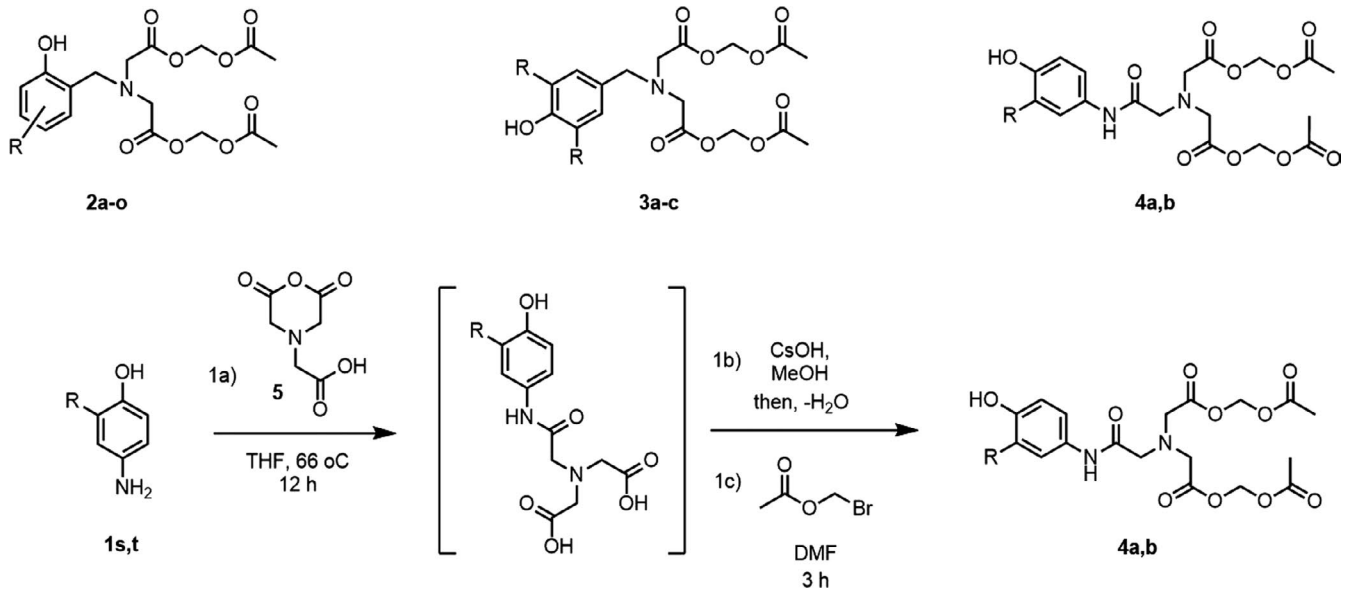

SCHEME 1 Phenolic iminodiacetate AM conjugates

antimicrobials to overcome biofilm tolerance has created an urgent need for novel, efficacious anti-biofilm agents.

Prodrug strategies have been effectively used to modify a wide array of structurally diverse pharmaceuticals to improve their physicochemical, pharmacokinetic, solubility, and biopharmaceutical properties, or to circumvent issues such as premature drug metabolism (Forde & Devocelle, 2015; Peeters et al., 2016; Pereira de Sousa & Bernkop-Schnurch, 2014; Rautio et al., 2008; Wu, 2009). This is achieved through the incorporation of bio-reversible functional groups, which will be cleaved enzymatically upon delivery of the drug to the active site. A variety of structurally diverse functional groups have been employed for this purpose, including phosphates, hemisuccinates, aryloxyphosphoramidates, phosphonooxymethyls, carbamates, aminoacyl conjugates, ethers, and esters (Patil et al., 2015; Ueda et al., 2003; Walther, Rautio, & Zelikin, 2017). To target a biofilm, an ideal prodrug would partition from the bulk aqueous phase into the biofilm, where it would be concentrated and retained. This functionality could allow a small amount of antimicrobial agent to be added to the bulk water and effectively deploy to biofilm-impacted surfaces.

Ester functional groups, in particular, are employed to enhance lipophilicity and thus membrane permeability (Beaumont, Webster, Gardner, & Dack, 2003; Ettmayer, Amidon, Clement, & Testa, 2004; Ma et al., 2017), and are used both in pharmaceuticals (Rautio et al., 2008) and intracellular fluorescent dyes such as Calcein blue AM (Huitink, Poe, & Diehl, 1974; Stabnis, 2010). This labile (acetoxy)methyl (AM) coumarin derivative passively crosses the cell membrane of viable cells where it is then converted by esterase cleavage into Calcein blue, which is retained within the cell as its Ca^{+2} chelate, without compromising the cell membrane (Bratosin, Mitrofan, Palii, Estaquier, & Montreuil, 2005; Davison, Pitts, & Stewart, 2010). Calcein dyes have also been shown to stain biofilms of both Gram-negative and Gram-positive bacteria such as *Streptococcus oralis*, *Streptococcus gordonii*, *S. mutans*, and *Pseudomonas aeruginosa* as well as endodontic biofilms (Herzog et al., 2017; Ohsumi et al., 2015; Perinbam & Siryaporn, 2018; Takenaka, Trivedi, Corbin, Pitts, & Stewart, 2008; Wakamatsu et al., 2014). We therefore elected to incorporate the "AM" group to modulate polarity and cellular retention to increase the antimicrobial potency of small phenols.

In this investigation, we demonstrate that the modest antibacterial activity of simple phenols can be markedly increased by the incorporation of iminodiacetate (acetoxy)methyl (AM) groups. Differences in potency between the parent phenols and prodrugs derivatives were evaluated against both planktonic cells and biofilms of the model bacteria *S. epidermidis* (35984) and *P. aeruginosa* (PA01). Both bacteria were chosen for their propensity to form biofilms (Büttner, Mack, & Rohde, 2015; Ciofu & Tolker-Nielsen, 2019; Sakimura et al., 2015) and prevalence in hospital-acquired infections (Maurice, Bedi, & Sadikot, 2018; Peleg & Hooper, 2010). We chose phenols as initial scaffolds to explore and demonstrate the AM prodrug strategy since phenols are traditional disinfectants and constituents of many antiseptic essential oils. A collection of simple phenols consisting of eugenol (Latifah-Munirah, Himratul-Aznita, & Mohd Zain, 2015) (**1f**), 4-fluorophenol (Zhao & Chen, 2016) (**1i**), 4-chlorophenol (Liu, Thomson, & Kaiser, 1982; Zhao & Chen, 2016) (**1j**), 2-methyl-4-chlorophenol (Oh et al., 2009) (**1k**), 2-methyl-4-nitrophenol (**4l**), capsaicin (Xing, Cheng, & Yi, 2006) (**1h**), and 2,6-dichlorophenol (Liu et al., 1982) (**1q**) were selected for their known antimicrobial properties. Several other phenols were also investigated for structure activity comparison.

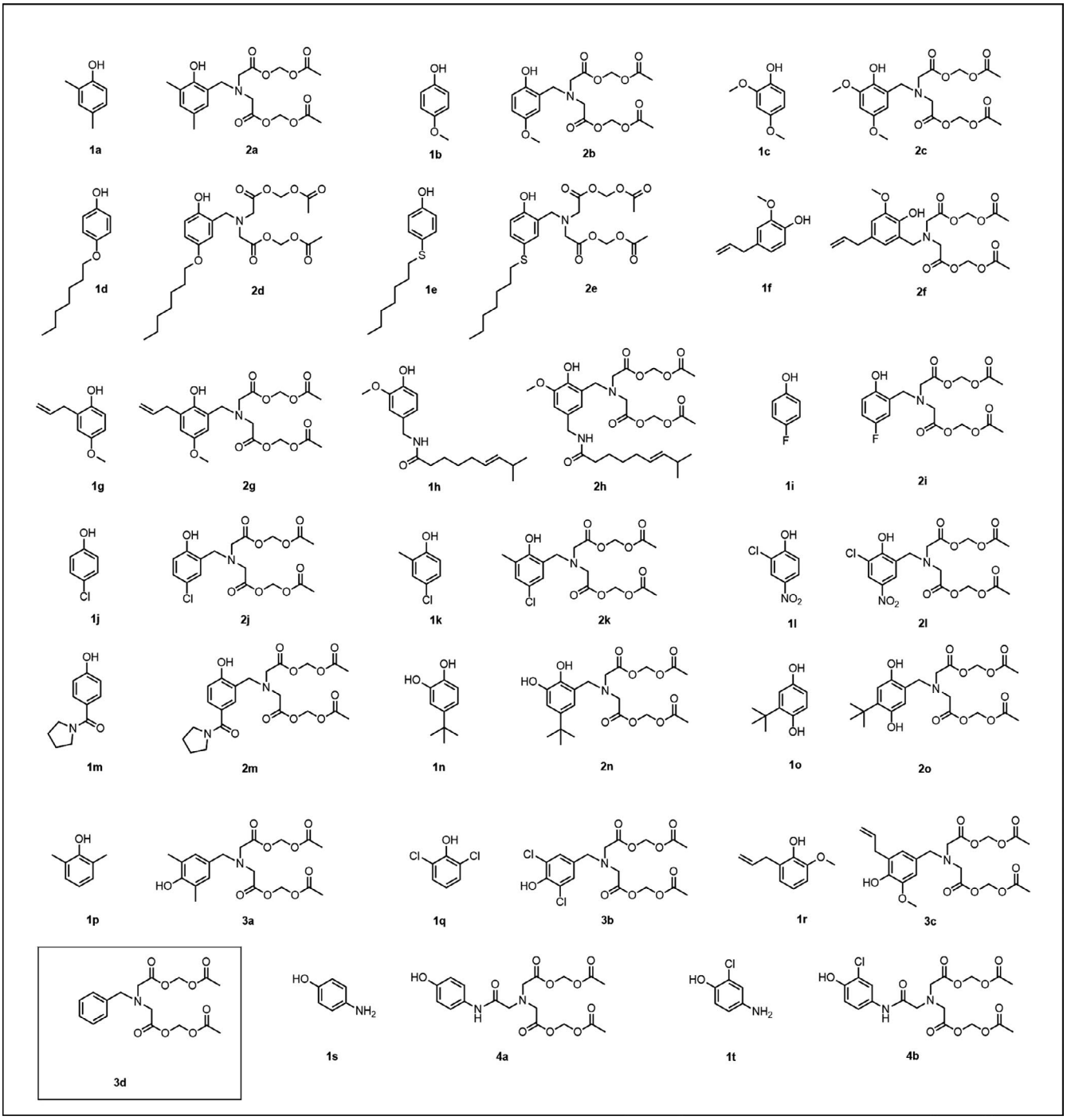

FIGURE 1 Parent phenols and AM derivatives

1.1 | Structural considerations

Parent phenols **1a–t** were transformed into three basic architectural motifs corresponding to the structures **2a–o**, **3a–c**, and **4a,b**. AM derivatives of the types **2** and **3** were prepared by modifications of the classical "phenol-Mannich" condensation (d'Hardemare, Jarjayes, & Mortini, 2004; Marzec, Zhang, Zhu, & Schmitt, 2017). The AMs **4a** and **4b** were synthesized by acylation of the corresponding phenols with anhydride **5** followed by cesium salt formation and alkylation with bromomethyl acetate (Scheme 1). The direct use of anhydride **5** as a vehicle for the facile assembly of AM bearing chelation constructs is noteworthy. It should be a straightforward proposition to employ this strategy for incorporating *alternative* antimicrobials in prodrug scaffolds.

2-Substituted phenolic iminodiacetates are well-known for forming chelate structures where the hydroxyl function is ligated to the metal cation (i.e., Ca^{+2}; d'Hardemare et al., 2004; Huitink et al., 1974; Kerber, Goheen, Perez, & Siegler, 2016; Marzec et al., 2017; Schwarzenbach,

Sallmann, & Komplexone, 1952; Stabnis, 2010; Tarn, Xue, & Zink, 2013). In contrast, for iminodiacetates corresponding to **3a–c** and **4a/b**, internal coordination of the phenolic hydroxyl would not be expected. Since the hydroxyl is likely responsible for antimicrobial activity, a comparison of instances where chelation is present (e.g., **2a–o**) to cases where this in not a factor (**3a–c** and **4a/b**) was considered an imperative. The phenols and their corresponding AM derivatives are assembled in Figure 1.

2 | METHODS AND MATERIALS

2.1 | Synthetic reagents and bacteria

All chemical reagents purchased for chemical synthesis were purchased from commercial sources and used as received without further purification, unless stated in the supplementary information. Solvents for filtrations, transfers, and chromatography were certified ACS grade. HEPES buffer and DE broth were purchased from Sigma. Thin-layer chromatography was performed on Silicycle Glass Backed TLC plates, and visualization was accomplished with UV light (254 nm), and/or potassium permanganate. All ^{1}H NMR spectra were recorded on a Bruker DRX300. All ^{13}C NMR spectra were recorded on a Bruker DRX500, and all NMR data were reported in ppm, employing the solvent resonance as the internal standard. High-resolution mass spectra (HRMS) were obtained with a Bruker micrOTOF-II.

Pseudomonas aeruginosa (PA01 and PA015542) and *S. epidermidis* (35984) were obtained from American Type Culture Collection (ATCC). All bacteria were sub-cultured onto tryptic soy agar (TSA) plates and incubated at 37°C for 24 hr. Single colonies were transferred from the plates and inoculated into 25 ml tryptic soy broth (TSB) in Erlenmeyer flasks. Culture were incubated 37°C for 24 hr and 10 μl of culture was transferred into 25 ml of TSB, and the absorbance was read at 600 nm using a spectrophotometer and standardized to 10^6–10^7 CFU/ml.

2.2 | Efficacy of naturally occurring phenols and derivatives on inhibiting planktonic cells

The minimum inhibitory concentrations (MICs) of all compounds against *S. epidermidis* and *P. aeruginosa* were determined using a modified 96-well plate assay previously described by Xie, Singh-Babak, and Cowen (2012). In short, both strains were cultured as described above in TSB and 150 μl of culture at an optical density to 0.05 at 600 nm was aliquoted into the wells of 96-well plates along with 150 μl of the compound being evaluated in DMSO. Plates were incubated at 37°C for 24 hr in static conditions. The optical density was taken via microplate reader at 0 hr and at 24 hr, and the difference measured to determine the MIC. Data from at least three replicates were evaluated for each compound tested. The same starting concentration of each compound was used for each replicate, and for this reason there is no standard error. Samples were diluted in dimethyl sulfoxide (DMSO), and DMSO controls were also conducted. Experiments were done in biological triplicate with technical duplicates.

2.3 | Efficacy of naturally occurring phenols and derivatives on biofilms

2.3.1 | Minimum Biofilm Eradication Concentration plate assays

Both strains were cultured as described above, and biofilms were grown in Costar polystyrene 96-well plates at 37°C. After 24 hr of incubation, without shaking, the planktonic phase cells were gently removed and the wells washed three times with PBS. Wells were filled with 150 μl dilutions of the compound being evaluated. The 96-well plates were incubated for an additional 24 hr at 37°C. The medium was gently removed and each well filled with 150 μl PBS and the biofilm broken up through stirring with sterile, wooden rods. Three tenfold dilutions of each sample were taken and drop plated on TSA plates and incubated for 24 hr. The Minimum Biofilm Eradication Concentration (MBEC) was determined to be the lowest concentration at which no bacterial growth occurred. The same starting concentration of each compound was used for each replicate, and for this reason there is no standard error. This procedure was modelled based on previously reported procedures according to Pitts, Hamilton, Zelver, and Stewart (2003). Experiments were done in biological triplicate with technical duplicates.

2.3.2 | Center for disease control (CDC) biofilm reactor evaluation

A CDC biofilm reactor was also used to assess potency of compounds toward biofilms. American Society for Testing and Materials (ASTM) method E2562-17, which describes how to grow a biofilm in the CDC biofilm reactor under high shear and continuous flow, and ASTM method E2871-13, a biofilm efficacy test generally known as the single tube method was used for this procedure. Formation of 48 hr biofilms in a CDC reactor was done on glass coupons (4.02 cm^2). A CDC reactor containing 340 ml of TSB (300 mg/L) was inoculated with 1 ml of a 3.21×10^8 CFU/ml overnight culture of *P. aeruginosa* (PA015542), which was grown in TSB

(300 mg/L) overnight. The biofilm was grown in batch mode at room temperature stirring at 125 rpm for 24 hr to establish the biofilm and then for 24 hr at room temperature under continuous flow with a feed rate of 11.25 ml/min at 125 rpm. The continuous feed TSB concentration was 100 mg/L. Coupons were then sampled from the reactor in triplicate. The mean log reduction in viable biofilms cells exposed to each compound for 1 hr was quantitatively measured according to ASTM method E2871-13. After coupons were removed from the CDC reactor, they were rinsed and transferred to separate 50 ml conical tubes and 4 ml of a 100 mM solution of the antimicrobial compound being tested in sterile PBS buffer was added. The tubes were incubated at room temperature under static conditions for 1 hr. After 1 hr, 36 ml Dey–Engley neutralizing (DE) broth was added and the biofilm was disaggregated by a series of vortexing and sonicating for 30 s each in the order of v/s/v/s/v. Each sample was diluted tenfold six times and the diluted samples were drop plated on Reasoner's 2A agar (R2A) agar plates, incubated overnight at 37°C and enumerated. Experiments were done in biological triplicate with technical duplicates. The mean log reduction was determined for each compound evaluated using the following equation:

$$\text{Log reduction} = \log 10\left(\frac{A}{B}\right)$$

where A is the average number of CFU before treatment and B is the average number of CFU after treatment.

2.4 | Enzyme assay

A 30-microliter solution of bis(acetoxymethyl) 2,2′-((−2-hydroxy-5-methoxybenzyl)azanediyl)diacetate (**2b)** at a concentration of 50 μM in acetonitrile was dissolved in a 100 μl solution of esterase (from porcine liver 72 units/ml in cold HEPES buffer, pH 7.9). The mixture was incubated at 37°C for the either 8, 16, or 24 min and then cooled to 0°C to inhibit further enzyme activity. The sample was then extracted several times with acetonitrile and analyzed via LCMS, without the solvent being evaporated, to determine whether the cleaved product was present.

2.5 | Representative chemical synthesis procedures

2.5.1 | 2,2′-(2-Hydroxy-3-methoxy-5-allylbenzylazanediyl)diacetic acid (6g)

A 100 ml round-bottomed flask equipped with a magnetic stirring bar N_2 inlet and reflux condenser was charged with iminodiacetic acid (4.0 g, 30.0 mmol) sodium hydroxide (2.46 g, 61.5 mmol) followed by water (30 ml). The reactant mixture was stirred until the solids had dissolved and then methanol (25 ml), eugenol (4.66 g, 30 mmol), and 37% aqueous formaldehyde (2.43 ml, 30 mmol) were added in succession. The reactant mixture was then heated under reflux under N_2 for 30 hr. The resulting solution was then cooled in an ice bath, and 37% aqueous hydrochloric acid (6.2 g, 62 mmol) was added dropwise with vigorous stirring Removal of the methanol in vacuo led to the precipitation of the product. Subsequent filtration of the resulting slurry followed by washing of the filter cake with water 5 × 10 ml) and suction drying provided the title compound as a white powder (7.86 g, 85%). **^{1}H NMR** (500 MHz, DMSO-D_6): δ 6.70 (s, 1H), 6.49 (s, 1H), 5.92 (m, 1H), 5.03 (dd, J = 2.85 Hz, 2H), 3.80 (s, 2H), 3.73 (s, 3H), 3.41 (s, 4H), 3.24 (d, J = 4.02 Hz, 2H). **^{13}C NMR** (500 MHz, DMSO-D_6): δ 172.78, 147.89, 144.54, 138.54, 130.14, 121.93, 115.86, 112.58, 56.09, 54.52, 53.83. **HRMS** (**ESI**) calcd for $C_{15}H_{19}NO_6^-$ ($[M - H]^-$), 308.1212, found, 308.1275 g/mol.

2.5.2 | Diethyl 2,2′-(4-Hydroxy-3,5-dimethylbenzylazanediyl)diacetate

A 10 ml round-bottomed flask equipped with a magnetic stirring bar and a yellow gas-tight cap was charged with diethyl iminodiacetate (568 mg, 3.0 mmol), 2,6-dimethylphenol (366.5 mg, 3.0 mmol), and paraformaldehyde (100 mg, 3.33 mmol). Anhydrous CH_3CN (0.5 ml) and triethylamine (34 mg, 0.30 mmol) were then added, and the reactant mixture was blanketed with N_2 and sealed. The reactant mixture was subsequently stirred at 75°C for 20 hr. Purification of the product was achieved by chromatography on silica gel (EtOAc/hexane for elution) to furnish the title compound (271 mg, 84%). **^{1}H NMR** (300 MHz, $CDCl_3$): δ 7.19 (s, 1H), 6.90 (s, 1H), 4.10 (q, J = 6.0, 4H), 3.69 (s, 2H), 3.45 (s, 4H), 2.16 (s, 6H), 2.23 (t, J = 6.0 Hz, 2H). **^{13}C NMR** (500 MHz, $CDCl_3$): δ 170.70, 156.92, 155.04, 153.46, 122.20, 117.35, 115.75, 61.14, 55.81, 53.87 14.16. **HRMS** (**ESI**) calcd for $C_{17}H_{25}NO_5^+$ ($[M + H]^+$), 324.1733, found, 324.1806 g/mol.

2.5.3 | 2,2′-(4-Hydroxy-3,5-dimethylbenzylazanediyl)diacetetic acid (6a)

The *crude* phenolic iminodiester was dissolved in methanol (5 ml) and transferred to a 25 ml round-bottomed flask equipped with a magnetic stirring bar. The stirred solution was cooled to 0°C and 8 M aqueous NaOH (1.5 ml, 12 mmol) was added dropwise by syringe. The resultant mixture was stirred for 22 hr at r.t. and then cooled with stirring using an ice bath. Neutralization was then performed by the dropwise addition of

37% aqueous HCl (1.2 g, 12 mmol) after which the methanol was removed in vacuo. The residue was washed with water (2 × 5 ml) and then dried in vacuo. Trituration of the residue with 2/1 CH_3CN/THF (4.0 ml) resulted in the formation of a fine powder, which was filtered and washed with water (3 × 2 ml) to provide the above iminodiacid as a powder, which was dried in vacuo (208 mg, 78%). **^{1}H NMR** (500 MHz, DMSO-D_6): δ 6.84 (s, 1H), 6.61 (s, 1H), 3.78 (s, 2H), 3.41 (s, 4H) 2.14 (s, 3H), 2.10 (s, 3H). **^{13}C NMR** (500 MHz, DMSO-D_6): δ 172.90, 153.08, 131.14, 128.09, 127.09, 124.15, 212.46, 55.51, 53.07, 20.48, 16.18. **HRMS** (**ESI**) calcd for $C_{13}H_{17}NO_5^-$ ($[M-H]^-$), 266.1107, found, 266.1140 g/mol.

2.5.4 | Di(Acetoxy)methyl N-(3-Chloro-4-hydroxyphenyl-1-aminoethanamide)-*N*,*N*-diethanoate (4b)

A 25 ml round-bottomed flask equipped with a magnetic stirring bar N_2 inlet and reflux condenser was charged with 2-chloro-4-aminophenol (143.6 mg, 1.0 mmol), morpholine-1-(acetic acid)-2,6-dione **5** (173.0 mg, 1.0 mmol), and anhydrous THF (5 ml). The stirred reactant mixture was heated at reflux for 12 hr, cooled, and the solvent was removed in vacuo to provide the product as a buff solid in quantitative yield. Methanol (3 ml) was added followed by 50% aqueous cesium hydroxide (610 mg, 2 mmol). The reactant mixture was stirred for 10 min to attained homogeneity. The resulting mixture was concentrated in vacuo, and the yellow solid was thoroughly dried under high vacuum at 60°C to provide the corresponding dicesium salt in quantitative yield. Anhydrous DMF (3 ml) was added to the flask, and the stirred reactant mixture was cooled to 0°C using an ice bath. Bromomethyl acetate (322 mg, 199 µl, 2.1 mmol) was added in a dropwise fashion. The reactant mixture was stirred for an additional 12 hr at 23°C as the suspended solid became a fine white precipitate. The resulting mixture was diluted with EtOAc (15 ml) and extracted with "half-saturated" brine (3 × 7 ml). The organic layer was subsequently dried with brine and then concentrated in vacuo. Purification of the residue by chromatography on silica gel (EA/Hex 1:1 for elution) provided the title compound (341 mg, 74%). **^{1}H NMR** (500 MHz, $CDCl_3$): δ 7.55 (s, 1H), 7.28 (d, J = 7.4 Hz, 1H), 6.82 (d, J = 7.4 Hz, 1H), 5.82 (s, 4H), 3.74 (s, 4H), 3.53 (s, 2H), 2.14 (s, 6H). **^{13}C NMR** (500 MHz, $CDCl_3$): δ 170.2, 169.58, 168.43, 153.03, 146.28, 130.45, 129.31, 121.44, 115.67, 79.51, 59.90, 55.91, 20.66. **HRMS** (**ESI**) calcd for $C_{18}H_{21}ClN_2O_{10}^+$ ($[M+H]^+$), 460.0885, found, 460.1330 g/mol.

3 | RESULTS AND DISCUSSION

In an initial study presented here, the minimum inhibitory concentrations (MIC) and biofilm eradication concentrations (MBEC) were evaluated for all parent phenols and their AM derivatives toward the Gram-negative bacterium *P. aeruginosa* and the Gram-positive bacterium *S. epidermidis*. AM derivatives were typically more potent than their corresponding parent phenols against planktonic cells, apart from **1/2k** against *S. epidermidis* (Table 1). We have previously shown that the lipophilic phenols **1d** (in particular) and **1e** are unusually potent toward *S. epidermidis* (Walsh et al., 2020). The observation that **2d** exhibits a lower potency compared to **1d** toward both bacteria may simply be a case where the exceptional activity of the parent phenol is ineffectively expressed in its AM. On the high end (average over four pairings), AM derivatives were 66 times more potent than their phenolic counterparts toward *S. epidermidis* and 16.0 times more potent toward *P. aeruginosa* in the planktonic phase. These results are consistent with the cleavage of the AM group via intracellular esterase, resulting in cellular retention and intracellular concentration of the phenolic antimicrobial.

Against biofilms, AMs were again more potent than parent phenols with rare exception. Toward biofilms, AM derivatives (high-end average over four pairings) were 9.3 times more potent toward *S. epidermidis* and 15.0 times more potent against *P. aeruginosa*. These results provide further

TABLE 1 MICs for parent phenols and respective AM derivatives against *S. epidermidis* and *P. aeruginosa*

Minimum inhibitory concentration (mM)				
	S. epidermidis		*P. aeruginosa*	
Compound	**Phenol**	**AM**	**Phenol**	**AM**
1/2a	1.9	0.1	1.9	0.5
1/2b	3.9	0.9	7.8	1.9
1/2c	15.6	0.23	7.8	1.9
1/2d	0.3	1.9	1.5	3
1/2e	4.5	1.9	7.8	3
1/2f	15.62	0.7	31.2	1.3
1/2g	7.9	0.5	15.6	1.3
1/2h	15.6	1.9	15.6	3.8
1/2i	15.6	0.1	7.8	0.9
1/2j	2.5	0.25	6.2	0.9
1/2k	0.9	1.5	1.9	0.75
1/2l	0.9	0.7	1.9	1.5
1/2m	15.6	7.8	31.2	25
1/2n	0.23	0.12	7.8	0.9
1/2o	0.23	0.023	3.9	0.5
1p/3a	1.9	0.5	1.9	0.1
1q/3b	3.1	0.6	3.9	0.9
1r/3c	125	62.5	125	31.2
1s/4a	15.6	3.9	15.6	1.9
1t/4b	7.8	1.9	15.6	3.9

confirmation that the addition of an AM group can substantially increase the modest potency of small phenols toward both biofilms and planktonic cells. It should be emphasized here that the foregoing results strongly support the use of an AM-based prodrug approach for increasing antimicrobial activities, even though the present compounds are active at high micro/low millimolar concentrations. It is expected that the potencies of commercially successful antimicrobials will be similarly augmented by the use of this strategy.

AMs **2c**, **2f**, **2j**, and **3b** were the most potent compounds against *S. epidermidis* biofilms, while AMs **2f**, **2k**, **2j**, and **3a** were most effective in eradicating *P. aeruginosa* biofilms. Exceptions to the predominant trend are **1/2k**, **1/2g**, and **1/2e** where parent and AM shared the same MBEC against *S. epidermidis* and compound **2d** where the AM was less potent against both bacteria (Table 2). In the cases of **1/2d**, **1/2e**, and **1/2k** (a chlorophenol), the parent phenol already possessed superb activity, with **2d** and **2e** sharing a highly hydrophobic substituent at the 4-position (vide supra; Walsh et al., 2020).

As a control experiment, AM **3d**, *which lacks a phenolic OH*, was among the least potent AM derivatives, with a MBEC of 24 mM toward both bacteria. It should be noted that many of these AMs possess electron rich aromatic nuclei (i.e., **2c** [for *S. epidermidis*], **2f** and **3a**) whereas the other is the simple 4-chloro derivative **2j**. The unexpectedly high activity of **2f** prompted us to investigate capsaicin derivative **2h**, to probe for a vanilloid receptor component. Unfortunately, **2h** was in no way special in its activity.

It is also interesting to note that the most potent parent phenols did not consistently result in the most potent AMs against biofilms. Phenols **1d**, **1e**, **1k**, **1j**, and **1q** were most potent toward *S. epidermidis*, while phenols **1d**, **1h**, **1k**, **1j**, and **1q** were most potent toward *P. aeruginosa* (Tables 1 and 2). Out of these six compounds, the only AMs with top potency were **2k** and **2j** toward *S. epidermidis*, with **2j** and **3b** most active toward *P. aeruginosa*. Phenol **1f** was among the least potent toward both bacteria while **2f** was among the five most potent toward both bacteria.

AMs **2f** and **2j** were the most successful compounds against biofilms for both types of bacteria. Two isomers of **2f**, **2g**, and **3c** were also evaluated. However, these isomers demonstrated a substantial decrease in potency compared to **2f**. This trend was not seen in parent phenols where **1g** was the most potent isomer toward *S. epidermidis* and **1r** was the most potent isomer toward *P. aeruginosa*. In parent phenols, a dramatic difference in potency was not observed as it was with the prodrug derivatives (Table 3).

These results suggest that the positioning of functional groups around the aromatic ring can make a dramatic difference in potency for AM derivatives, which is also observed in the isomers **2a** and **3a** (Table 3). AM **2a** has methyl groups is the 2 and 4 position while **3a** has methyl groups in the 2 and 6 positions. Here, **2a** is more potent toward *S. epidermidis* and **3a** more potent toward *P. aeruginosa* (Table 3). This was also observed with the corresponding phenols (Table 2).

It was observed that all compounds exhibited a higher potency toward planktonic cells when compared to biofilms (Tables 1 and 2). Parent phenols were, on average, 26 times more potent toward *S. epidermidis* planktonic cells compared

TABLE 2 MBECs for parent phenols and respective AM derivatives against *S. epidermidis* and *P. aeruginosa* determined via Minimum Biofilm Eradication Concentration plate assay

	Minimum Biofilm Eradication Concentration (mM)			
	S. epidermidis		*P. aeruginosa*	
Compound	**Phenol**	**AM**	**Phenol**	**AM**
1/2a	31.2	6.2	62.5	12.5
1/2b	31.2	12.5	31.2	12.5
1/2c	31.2	3.1	62.5	6.2
1/2d	1.9	12.6	7.5	25
1/2e	6.2	6.2	50	25
1/2f	31.2	2.7	62.5	2.7
1/2g	15.6	15.6	62.5	15.6
1/2h	25	7.8	25	15.6
1/2i	62.5	6.2	31	12.5
1/2j	3.1	2.7	6.2	3.1
1/2k	6.2	6.2	12.5	3.1
1/2l	31	7.8	31.2	12.5
1/2m	50	12.6	50	15.6
1/2n	15.6	7.8	31.2	15
1/2o	31.2	7.8	62.5	15
1p/3a	62.5	25	31.2	1.5
1q/3b	6.2	3	12.5	6.2
1r/3c	62.5	31.2	31.2	15.6
1s/4a	50	15.6	100	15.6
1t/4b	25	7.8	25	12.5

TABLE 3 MBECs for sets of isomers **2f**, **2g**, and **3c** as well as **2a** and **3a as** determined via Minimum Biofilm Eradication Concentration plate assay

Minimum Biofilm Eradication Concentration (mM)			
S. epidermidis		*P. aeruginosa*	
2a	6.2	**3b**	12.5
2f	2.7	**1b**	2.7
2g	15.6	**10b**	15.6
3a	25	**11b**	1.5
3c	31.2	**12b**	15.6

to biofilms and 10 times more potent toward *P. aeruginosa* in the planktonic state. AM derivatives were on average 55 times more potent toward planktonic *S. epidermidis* and 11 times more potent toward planktonic *P. aeruginosa* compared to the corresponding biofilm states. This was expected due to the higher susceptibility of planktonic cells. AMs also experienced a larger disparity in potencies between planktonic cells and biofilms than were seen with parent phenols. The latter observation is consistent with the ability for the cleaved iminodiacetate to concentrate within cells, a characteristic that the parent phenol lacks.

From a structural prospective, the AM series **3a–c**, wherein the phenolic OH occupies the 4-position, did not consistently show either a heightened or muted potency compared to **2a–o**, where involvement of the phenolic OH in chelation is expected (vide supra). It is nonetheless significant that both **3a** and **3b** exhibited a dramatic increase in potency toward *P. aeruginosa*. Interestingly, the "non-traditional" AMs **4a** and **b** did not show enhanced potency toward either bacteria compared to the five most potent "traditional" AMs. This could be due to the lengthened distance of the chelating moiety from the aromatic ring. As before, however, aromatic chlorine substitution did lead to an enhancement of activity (**4b** vs. **4a**, Table 4) as would be expected (Suter, 1941).

3.1 | Comparison of AM prodrugs to commercial antibiotics

Gratifying as the aforementioned activity enhancements were for the prodrug AMs *vis a vis* their parent phenols, overall potencies seldom reached the micromolar range expected for modern antibiotics against planktonic cells. To document a *direct* comparison to the present AMs, three commercial antibiotics were selected for MBEC evaluation under the current assay toward *S. epidermidis* and *P. aeruginosa* biofilms (Table 4). Metronidazole is a nitroimidazole derivative that was selected for its use in treating a variety of bacterial infections and has been shown to exhibit activity toward biofilms of *Helicobacter pylori* (Yonezawa, Osaki, Hojo, & Kamiya, 2019) and *C. difficile* (Vuotto, Moura, Barbanti, Donelli, & Spigaglia, 2016). Metronidazole had a MBEC of 6.2 mM toward *S. epidermidis* and 50 mM toward *P. aeruginosa* biofilms. Tobramycin is an aminoglycoside that was chosen because it has been extensively studied for efficacy toward *P. aeruginosa* biofilms and has been clinically used in the treatment of cystic fibrosis (Høiby et al., 2019). Under our experimental protocol, tobramycin had a MBEC of 18 mM toward *S. epidermidis* and of 0.06 mM toward *P. aeruginosa* biofilms. Nitazoxanide is a broad spectrum antiparasitic and antiviral drug that has more recently been studied for effectiveness against bacteria (Carvalho, Lin, Jiang, & Nathan, 2009; Guttner, Windsor, Viiala, Dusci, & Marshall, 2003; Singh & Narayan, 2011). Nitazoxanide has also been shown to inhibit S. epidermidis biofilm formation (Tchouaffi-Nana et al., 2010). Nitazoxanide demonstrated an MBEC of 50 mM toward *S. epidermidis* and of 3.12 mM toward *P. aeruginosa* biofilms.

Against *S. epidermidis* biofilms, several AM compounds were more potent than metronidazole and tobramycin. A comprehensive table (Table S1) can be found in the supplementary. All 18 AM prodrugs exhibited a lower MBEC toward *P. aeruginosa* when compared to metronidazole although here, tobramycin exhibited the highest potency of all compounds evaluated. Similarly, all 18 AM derivatives were more potent toward *S. epidermidis* when compared to nitazoxanide. That several AMs were more potent toward both bacteria compared to metronidazole might be anticipated since metronidazole is used to treat anaerobic infections while both *S. epidermidis* and *P. aeruginosa* are both facultative anaerobes.

In an additional control study, a selected number of iminodiacetic acids **5a**, **5g**, **5k**, and **5l** were evaluated for potency. These are the cleaved form of the drug, produced after esterase cleavage (Figure 2). The free iminodiacetates were not expected to effectively permeate through the biofilms or cross the cell membrane as efficiently as their AM counterparts.

All iminodiacetates were significantly less potent than their corresponding AM prodrugs against biofilms (Table 5). AMs were, on average, 10 times more potent than the corresponding iminodiacetates against *S. epidermidis* and 16 times more potent against *P. aeruginosa* biofilms. This also supports that the AM form of the drug is able to penetrate and eradicate cells within a biofilm. In comparison to phenols **5a**, **5g**, **5k**, and **5l**, it was also observed that the corresponding iminodiacetates were often less potent (Tables 1 and 5).

In effort to better explore additional synthetic options for derivations of iminodiacetate functionalized prodrugs, five variations of ester prodrugs (e.g., **6-10f**) were synthesized and evaluated against planktonic cells and biofilms. This was done in an effort to explore alternative ester varieties as prodrugs. Eugenol (**1f**) was chosen as the phenolic scaffold since its AM (**2f**) was one of the five most potent

TABLE 4 MBECs of 4-phenolic AMs as determined via Minimum Biofilm Eradication Concentration plate assay

	Minimum Biofilm Eradication Concentration (mM)			
	S. epidermidis		*P. aeruginosa*	
Compound	**Phenol**	**AM**	**Phenol**	**AM**
1p/3a	62.5	25	31.2	1.5
1q/3b	6.2	3	12.5	6.2
1r/3c	62.5	31.2	31.2	15.6
1s/4a	50	15.6	100	15.6
1t/4b	25	7.8	25	12.5

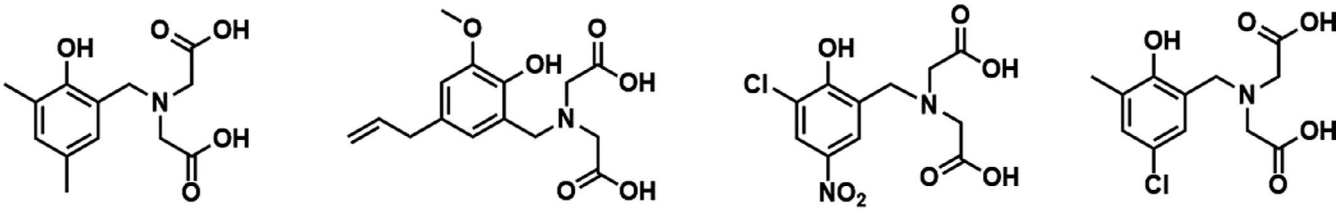

FIGURE 2 Phenolic iminodiacetic acids

TABLE 5 MBECs for AM prodrugs and cleaved iminodiacetic acids against *S. epidermidis* and *P. aeruginosa* determined via Minimum Biofilm Eradication Concentration plate assay

	Minimum Biofilm Eradication Concentration (mM)					
	S. epidermidis			*P. aeruginosa*		
Compound	Parent phenol	AM	Iminodiacid (5)	Parent phenol	AM	Iminodiacid (5)
1/2/5a	31.2	6.2	125	62.5	12.5	>250
1/2/5f	31.2	2.7	62.5	62.5	2.7	125
1/2/5k	6.2	6.2	62.5	12.5	3.1	125
1/2/5l	31	7.8	62.5	31.2	12.5	31.2

toward biofilms in the initial series (Table 1, vide supra). The hemiacytal MEM derivative **10f** was selected to increase hydrophilicity, since eugenol itself has low water solubility. The simple esters **6/7f** were selected since common ester functionality should be more robust toward esterase than the acylal function present in AMs. Acylals **8/9f** possess butyryl and pivaloyl esters in place of the acetate, respectively. These were selected for examining terminus variation of the iminodiacetate group. The bis(pivaloyloxy) methyl ester was also selected due to its use in prodrugs to improve bioavailability (Brass, 2002).

Against planktonic cells, prodrug derivative **8f** exhibited the highest potency against *S. epidermidis*, while **2f** showed the highest potency toward *P. aeruginosa* (Table 6). The ethyl and allyl ester derivatives (**6f**, **7f**) were the least potent prodrugs overall with MICs of 31.2 mM toward both bacteria. Against *S. epidermidis* **6f** and **7f** were also less potent than the parent phenol (**1f**) (Figure 3).

Against biofilms, AM **2f** had the highest potency against both bacteria (Table 7). Compound **7b** was the least potent toward *S. epidermidis* while **7e** was the least potent toward *P. aeruginosa*. This suggests that AM **2f** is either more permeable to the biofilm or the ester bonds present in this group are more readily cleaved by esterase or both. It is also of interest that the hemiacytal **7b** showed commendable activity toward *S. epidermidis*.

A CDC Biofilm reactor assay was also used to substantiate the comparative efficacy of eugenol (**1f**) with its corresponding AM derivative (**2f**) against *P. aeruginosa* (PA015542). Here, unlike the static condition of the 96-well plate, biofilms were grown in a high shear environment. This method increases the biofilm adherence to the surface on which it is grown and causes the biofilm to produce a more robust EPS (Gloag, Fabbri, Wozniak, & Stoodley, 2020; Stoodley, Cargo, Rupp, Wilson, & Klapper, 2002). This method was chosen because it has been standardized by the ASTM. Similar to

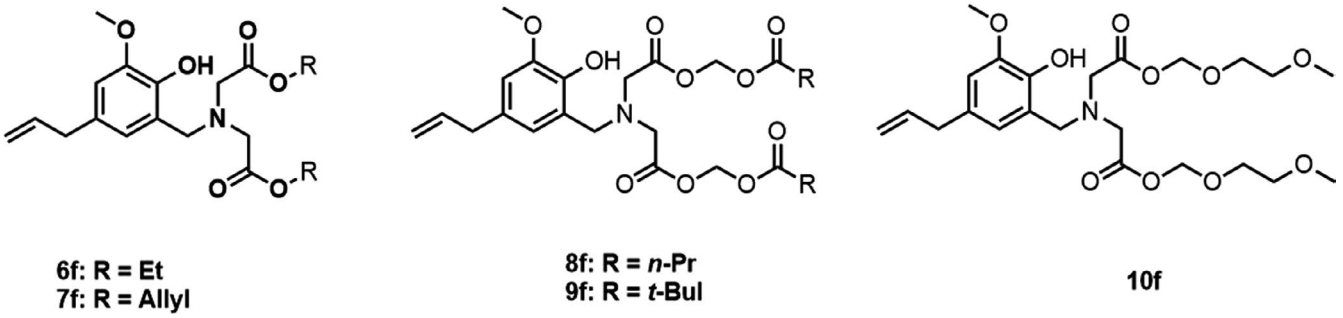

FIGURE 3 Alternative phenolic iminodiacetate esters

TABLE 6 MIC (mM) for eugenol (**1f**) and the alternative prodrug derivatives **7a**–**7e** compared to AM **2f**

Minimum inhibitory concentration (mM)			
S. epidermidis		*P. aeruginosa*	
1f	15.6	**1f**	31.2
2f	0.68	**2f**	1.3
6f	31.2	**6f**	31.2
7f	31.2	**7f**	31.2
8f	0.12	**8f**	3.9
9f	1.9	**9f**	15.6
10f	1.9	**10f**	31.2

the static 96-well plate assays, the potency of the AM derivative (**2f**) was greater than the parent compound (**1f**) using the CDC biofilm reactor. Eugenol (**1f**) demonstrated a mean log reduction of 1.68 ± 0.12 while its corresponding AM (**2f**) had a mean log reduction of 5.81 ± 0.53. A graph of these data can be found in the supplementary materials (Figure S1). This has shown that the AM (**2f**) is significantly more potent than the parent (**1f**) against biofilms grown in both static and high shear environments.

Once AMs have penetrated the biofilm's extracellular matrix and the membrane of indwelling cells, they are predicted to be acted upon by intracellular esterase, liberating the active form as the iminodiacetate. The resulting highly charged antimicrobial is then entrapped within the cell. The observed increase in potency supports that AMs are being acted upon by esterase once inside the cell, but additional experimentation was also performed to further support this hypothesis. According to KEGG genome annotations, *P. aeruginosa* (PAO1) and *S. epidermidis* (RP62A) contain 39 and 16 esterases, respectively, as well as other enzymes that have been shown to have esterase activity (Foster, 1996; Goullet & Picard, 1991). For example, EstA has been shown to possess esterase activity in *Pseudomonas* and is thought to be involved the hydrolysis of ester containing compounds

TABLE 7 MBEC (mM) for eugenol (**1f**) and the alternative prodrug derivatives **6–10f** compared to AM **2f**, determined via Minimum Biofilm Eradication Concentration plate assay

Minimum Biofilm Eradication Concentration (mM)			
S. epidermidis		*P. aeruginosa*	
1f	31.2	**1f**	62.5
2f	2.75	**2f**	2.75
6f	31.2	**6f**	62.5
7f	50	**7f**	50
8f	15.6	**8f**	62.5
9f	20.6	**9f**	41.2
10f	7.8	**10f**	125

on the cell surface or in the culture medium (Nicolay, Devleeschouwer, Vanderleyden, & Spaepen, 2012; Wilhelm, Gdynia, Tielen, Rosenau, & Jaeger, 2007). Here, esterase from porcine liver was used because it has been shown to readily cleave ester bonds in small organic molecules (Perez, Daniel, & Cohen, 2013) as well as antibiotics such as ampicillin and amoxicillin (Zhou et al., 2019). In order to determine whether esterase will cleave these AM groups, **2b** was exposed to esterase in vitro and samples were viewed via mass spectrometry to determine if the liberated iminodiacetate **5b** was present (Figure 4).

The AM derivative of 4-methoxyphenol (**2b)** was exposed to esterase in cold HEPES buffer, and LC-MS was performed to determine the amount of the liberated product, 2,2′-((2-hydroxy-5-methoxybenzyl)azanediyl)diacetate (**5b**), present. The exact mass of **2b** is 413.1322 amu, with a predicted $[M]^-$ of 413.1322 amu and the exact mass of **5b** is 267.0745 amu with predicted $[M - 2H]^{2-}$ of 132.5366 amu. The exact mass of the protonated derivative of **5b** is 269.0889 amu with a predicted $[M + H]^+$ of 268.0816. Both the mono- and di-anionic product are expected to be present in the esterase exposed samples, which were evaluated.

Spectra were taken of the pure AM compound **2b** (**A**) and the liberated derivative **5b** (**B**) (Figure 5). In frame **B**, both peaks for the mono and di-anionic species can be observed. The AM **2b** was exposed to esterase in HEPES buffer for 8 (**D**), 16 (**E**), and 24 (**F**) min, extracted, and then analyzed via LCMS (Figure 5). The masses of **2b** and **5b** were found were within two decimals of the predicted masses for each compound. A control of **2b** in HEPE without esterase was also included to ensure that HEPE does not influence the prodrug (**C**). This assay has shown that, in vitro, the AM derivatives are, in fact, acted upon by esterase. This suggests that the increase in potency is, in part, due to the AM being able to penetrate the biofilm and transform within the cell to release the iminodiacetate. This is further supported by the observation that the iminodiacetates **5a**, **5f**, **5k**, and **5l** are significantly less active than the corresponding AMs toward biofilms. Although an in vivo study has yet to be conducted, Calcein AM has been used extensively to successfully stain biofilms (Godoy-Santos, Pitts, Stewart, & Mantovani, 2019; Ohsumi et al., 2015; Tawakoli, Al-Ahmad, Hoth-Hannig, Hannig, & Hannig, 2013; Tawakoli et al., 2013; Wakamatsu et al., 2014) and the results presented herein strongly support the hypothesis that AM derived prodrugs will act via a similar mechanism.

4 | CONCLUSION

This investigation has shown that AMs (14 out of 18 AMs against *S. epidermidis* and 18 out of 18 AMs against *P. aeruginosa*) are often significantly more potent than

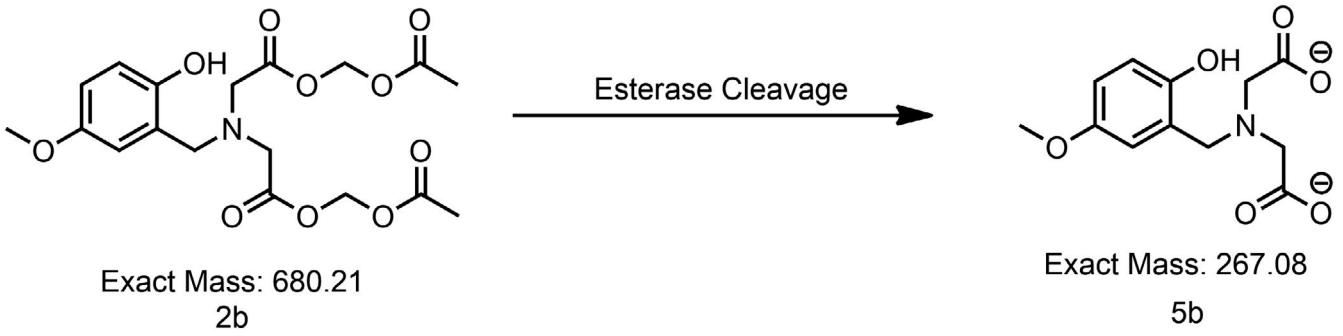

FIGURE 4 Esterase cleavage of AM 2b

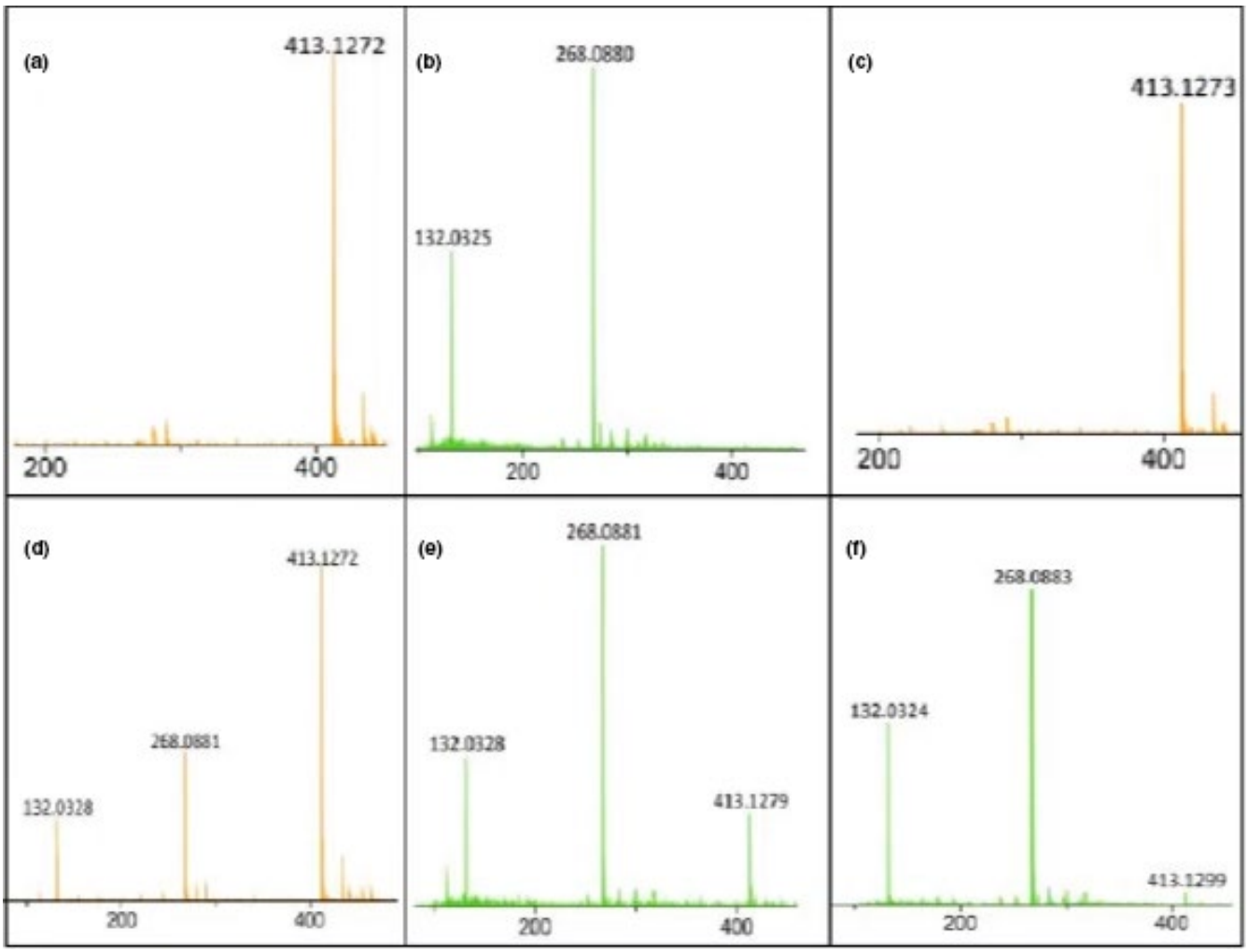

FIGURE 5 Liquid chromatography–mass spectrometry of parent AM **2b** before and after exposure to esterase run in negative mode. (a) Pure AM derivative **2b**, (b) pure protonated derivative of **8c** (c) **2b** after being exposed to HEPES buffer with no esterase, (d) **2b** after being exposed to esterase for 8 min in HEPES buffer, (e) **2b** after being exposed to esterase for 16 min in HEPES buffer, and (f) **2b** after being exposed to esteraes for 24 min in HEPES buffer [Colour figure can be viewed at wileyonlinelibrary.com]

corresponding parent phenols toward biofilm eradication. These results strongly support the use of an AM-based prodrug approach for increasing antimicrobial activities, even though the present compounds are active at high micro/low millimolar concentrations. It is therefore expected that the addition of an AM assembly will substantially increase the antibacterial potency of conventional antibiotics toward both planktonic cells and biofilms. On

the high end (average over four pairings), AM derivatives were 66 times more potent than their phenolic counterparts toward *S. epidermidis* and 16.0 times more potent toward *P. aeruginosa* in planktonic assays. Against biofilms, AM derivatives (high-end average) were 9.3 times more potent toward *S. epidermidis* and 15.0 times more potent against *P. aeruginosa*. Overall, AM planktonic averages were 25.40 times toward *S. epidermidis* and 8.44 times toward *P. aeruginosa*. In the case of biofilms, AMs were on average 2.9 times more potent toward *S. epidermidis* and 3.7 times more potent against *P. aeruginosa*. Metal cation chelation, to the extent that it may occur in iminodiacetates emergent from **2a**–**o**, appears to be a minor factor in the governance of antibacterial activity for *S. epidermidis*, but can suppress potency toward *P. aeruginosa* biofilms (e.g., **2a** vs. **3a**). In addition, we have developed an exceptionally direct method for the assembly of AM bearing pro-chelation motifs (i.e., **1** → **4**). The utilization of this, and related strategies, for the elaboration of AM prodrugs derived from *new* as well as commercial antimicrobials will be the topics of future accounts from these laboratories.

ACKNOWLEDGMENTS

Generous funding for this research was provided by the National Institute for General Medical Science grant number GM 116949.

CONFLICT OF INTEREST

The authors declare that there is no conflict of interest regarding the publication of this paper.

DATA AVAILABILITY STATEMENT

Supplementary information can be found here.

ORCID

Danica J. Walsh https://orcid.org/0000-0002-5509-1224

REFERENCES

Beaumont, K., Webster, R., Gardner, I., & Dack, K. (2003). Design of ester prodrugs to enhance oral absorption of poorly permeable compounds: Challenges to the discovery scientist. *Current Drug Metabolism*, *4*(6), 461–485.

Brass, E. P. (2002). Pivalate-generating prodrugs and carnitine homeostasis in man. *Pharmacological Reviews*, *54*(4), 589–598. https://doi.org/10.1124/pr.54.4.589

Bratosin, D., Mitrofan, L., Palii, C., Estaquier, J., & Montreuil, J. (2005). Novel fluorescence assay using calcein-AM for the determination of human erythrocyte viability and aging. *Cytometry Part A*, *66A*(1), 78–84. https://doi.org/10.1002/cyto.a.20152

Bryers, J. D. (2008). Medical biofilms. *Biotechnology and Bioengineering*, *100*(1), 1–18. https://doi.org/10.1002/bit.21838

Büttner, H., Mack, D., & Rohde, H. (2015). Structural basis of *Staphylococcus epidermidis* biofilm formation: Mechanisms and molecular interactions. *Frontiers in Cellular and Infection Microbiology*, *5*, 14.

Campanac, C., Pineau, L., Payard, A., Baziard-Mouysset, G., & Roques, C. (2002). Interactions between biocide cationic agents and bacterial biofilms. *Antimicrobial Agents and Chemotherapy*, *46*(5), 1469–1474. https://doi.org/10.1128/AAC.46.5.1469-1474.2002

Ciofu, O., & Tolker-Nielsen, T. (2019). Tolerance and resistance of *Pseudomonas aeruginosa* biofilms to antimicrobial agents-how *P. aeruginosa* can escape antibiotics. *Frontiers in Microbiology*, *10*, 913. https://doi.org/10.3389/fmicb.2019.00913

Conlon, B. P., Nakayasu, E. S., Fleck, L. E., LaFleur, M. D., Isabella, V. M., Coleman, K., … Lewis, K. (2013). Activated ClpP kills persisters and eradicates a chronic biofilm infection. *Nature*, *503*(7476), 365–370.

Costerton, J. W., Stewart, P. S., & Greenberg, E. P. (1999). Bacterial biofilms: A common cause of persistent infections. *Science (New York, N.Y.)*, *284*(5418), 1318–1322.

Davenport, E. K., Call, D. R., & Beyenal, H. (2014). Differential protection from tobramycin by extracellular polymeric substances from *Acinetobacter baumannii* and *Staphylococcus aureus* biofilms. *Antimicrobial Agents and Chemotherapy*, *58*(8), 4755–4761. https://doi.org/10.1128/AAC.03071-14

Davison, W. M., Pitts, B., & Stewart, P. S. (2010). Spatial and temporal patterns of biocide action against *Staphylococcus epidermidis* biofilms. *Antimicrobial Agents and Chemotherapy*, *54*(7), 2920–2927. https://doi.org/10.1128/AAC.01734-09

de Carvalho, L. P. S., Lin, G., Jiang, X., & Nathan, C. (2009). Nitazoxanide kills replicating and nonreplicating *Mycobacterium tuberculosis* and evades resistance. *Journal of Medicinal Chemistry*, *52*(19), 5789–5792.

d'Hardemare, A. M., Jarjayes, O., & Mortini, F. (2004). Solvent- and catalyst-free selective mannich reaction on catechols and para substituted phenols: A convenient route to catechol- and phenol-iminodiacetic acid ligands. *Synthetic Communications*, *34*(21), 3975–3988.

Donlan, R. M., & Costerton, J. W. (2002). Biofilms: Survival mechanisms of clinically relevant microorganisms. *Clinical Microbiology Reviews*, *15*(2), 167–193. https://doi.org/10.1128/CMR.15.2.167-193.2002

Ettmayer, P., Amidon, G. L., Clement, B., & Testa, B. (2004). Lessons learned from marketed and investigational prodrugs. *Journal of Medicinal Chemistry*, *47*(10), 2393–2404. https://doi.org/10.1021/jm0303812

Flemming, H. C., & Wingender, J. (2010). The biofilm matrix. *Nature Reviews. Microbiology*, *8*(9), 623–633. https://doi.org/10.1038/nrmicro2415

Flemming, H. C., Wingender, J., Szewzyk, U., Steinberg, P., Rice, S. A., & Kjelleberg, S. (2016). Biofilms: An emergent form of bacterial life. *Nature Reviews Microbiology*, *14*(9), 563–575. https://doi.org/10.1038/nrmicro.2016.94

Forde, E., & Devocelle, M. (2015). Pro-moieties of antimicrobial peptide prodrugs. *Molecules*, *20*(1), 1210–1227. https://doi.org/10.3390/molecules20011210

Foster, T. (1996). *Staphylococcus*. In S. Baron (Ed.), *Medical microbiology*, chapter 12. Galveston (TX): University of Texas Medical Branch at Galveston.

Gloag, E. S., Fabbri, S., Wozniak, D. J., & Stoodley, P. (2020). Biofilm mechanics: Implications in infection and survival. *Biofilm*, *2*, 100017. https://doi.org/10.1016/j.bioflm.2019.100017

Godoy-Santos, F., Pitts, B., Stewart, P. S., & Mantovani, H. C. (2019). Nisin penetration and efficacy against *Staphylococcus aureus* biofilms under continuous-flow conditions. *Microbiology (Reading, England)*, *165*(7), 761–771. https://doi.org/10.1099/mic.0.000804

Goullet, P., & Picard, B. (1991). *Pseudomonas aeruginosa* isolate typing by esterase electrophoresis. *FEMS Microbiology Letters*, *78*(2–3), 195–200. https://doi.org/10.1016/0378-1097(91)90157-6

Guttner, Y., Windsor, H. M., Viiala, C. H., Dusci, L., & Marshall, B. J. (2003). Nitazoxanide in treatment of Helicobacter pylori: A clinical and in vitro study. *Antimicrobial Agents and Chemotherapy*, *47*(12), 3780–3783.

Hall, C. W., & Mah, T. F. (2017). Molecular mechanisms of biofilm-based antibiotic resistance and tolerance in pathogenic bacteria. *FEMS Microbiology Reviews*, *41*(3), 276–301. https://doi.org/10.1093/femsre/fux010

Herzog, D. B., Hosny, N. A., Niazi, S. A., Koller, G., Cook, R. J., Foschi, F., … Festy, F. (2017). Rapid bacterial detection during endodontic treatment. *Journal of Dental Research*, *96*(6), 626–632. https://doi.org/10.1177/0022034517691723

Høiby, N., Henneberg, K.-Å., Wang, H., Stavnsbjerg, C., Bjarnsholt, T., Ciofu, O., … Sams, T. (2019). Formation of *Pseudomonas aeruginosa* inhibition zone during tobramycin disk diffusion is due to transition from planktonic to biofilm mode of growth. *International Journal of Antimicrobial Agents*, *53*(5), 564–573. https://doi.org/10.1016/j.ijantimicag.2018.12.015

Huitink, G. M., Poe, D. P., & Diehl, H. (1974). On the properties of Calcein Blue. *Talanta*, *21*(12), 1221–1229. https://doi.org/10.1016/0039-9140(74)80143-8

Kerber, W. D., Goheen, J. T., Perez, K. A., & Siegler, M. A. (2016). Enhanced stability of the Fe(II)/Mn(II) state in a synthetic model of heterobimetallic cofactor assembly. *Inorganic Chemistry*, *55*(2), 848–857.

Khatoon, Z., McTiernan, C. D., Suuronen, E. J., Mah, T.-F., & Alarcon, E. I. (2018). Bacterial biofilm formation on implantable devices and approaches to its treatment and prevention. *Heliyon*, *4*(12), e01067. https://doi.org/10.1016/j.heliyon.2018.e01067

Kim, S. J., Moon, D. C., Park, S. C., Kang, H. Y., Na, S. H., & Lim, S. K. (2019). Antimicrobial resistance and genetic characterization of coagulase-negative staphylococci from bovine mastitis milk samples in Korea. *Journal of Dairy Science*, *102*(12), 11439–11448. https://doi.org/10.3168/jds.2019-17028

Latifah-Munirah, B., Himratul-Aznita, W. H., & Mohd Zain, N. (2015). Eugenol, an essential oil of clove, causes disruption to the cell wall of *Candida albicans* (ATCC 14053). *Frontiers in Life Science*, *8*(3), 231–240.

Liu, D., Thomson, K., & Kaiser, K. L. E. (1982). Quantitative structure-toxicity relationship of halogenated phenols on bacteria. *Bulletin of Environmental Contamination and Toxicology*, *29*(2), 130–136. https://doi.org/10.1007/BF01606140

Ma, J., Wu, S., Zhang, X., Guo, F., Yang, K., Guo, J., … Du, Y. (2017). Ester prodrugs of IHVR-19029 with enhanced oral exposure and prevention of gastrointestinal glucosidase interaction. *ACS Medicinal Chemistry Letters*, *8*(2), 157–162. https://doi.org/10.1021/acsmedchemlett.6b00332

Malheiro, J., & Simões, M. (2017). 4 - Antimicrobial resistance of biofilms in medical devices. In Y. Deng, & W. Lv (Eds.), *Biofilms and implantable medical devices* (pp. 97–113). Cambridge, UK: Woodhead Publishing.

Marzec, B., Zhang, L., Zhu, N., & Schmitt, W. (2017). Bio-inspired synthetic approaches: From hierarchical, hybrid supramolecular assemblies to $CaCO_3$-based microspheres. *Dalton Transactions*, *46*(19), 6456–6463.

Maurice, N. M., Bedi, B., & Sadikot, R. T. (2018). *Pseudomonas aeruginosa* biofilms: Host response and clinical implications in lung infections. *American Journal of Respiratory Cell and Molecular Biology*, *58*(4), 428–439.

Nicolay, T., Devleeschouwer, K., Vanderleyden, J., & Spaepen, S. (2012). Characterization of esterase A, a *Pseudomonas stutzeri* A15 autotransporter. *Applied and Environmental Microbiology*, *78*(8), 2533–2542. https://doi.org/10.1128/AEM.07690-11

Oh, K.-B., Lee, J. H., Lee, J. W., Yoon, K.-M., Chung, S.-C., Jeon, H. B., … Lee, H.-S. (2009). Synthesis and antimicrobial activities of halogenated bis(hydroxyphenyl)methanes. *Bioorganic & Medicinal Chemistry Letters*, *19*(3), 945–948. https://doi.org/10.1016/j.bmcl.2008.11.089

Ohsumi, T., Takenaka, S., Wakamatsu, R., Sakaue, Y., Narisawa, N., Senpuku, H., … Okiji, T. (2015). Residual structure of *Streptococcus mutans* biofilm following complete disinfection favors secondary bacterial adhesion and biofilm re-development. *PLoS One*, *10*(1), e0116647. https://doi.org/10.1371/journal.pone.0116647

Patil, S., Lis, L. G., Schumacher, R. J., Norris, B. J., Morgan, M. L., Cuellar, R. A., … Georg, G. I. (2015). Phosphonooxymethyl prodrug of triptolide: Synthesis, physicochemical characterization, and efficacy in human colon adenocarcinoma and ovarian cancer xenografts. *Journal of Medicinal Chemistry*, *58*(23), 9334–9344. https://doi.org/10.1021/acs.jmedchem.5b01329

Peeters, E., Hooyberghs, G., Robijns, S., Waldrant, K., De Weerdt, A., Delattin, N., … Steenackers, H. P. (2016). Modulation of the substitution pattern of 5-aryl-2-aminoimidazoles allows fine-tuning of their antibiofilm activity spectrum and toxicity. *Antimicrobial Agents and Chemotherapy*, *60*(11), 6483–6497. https://doi.org/10.1128/AAC.00035-16

Peleg, A. Y., & Hooper, D. C. (2010). Hospital-acquired infections due to gram-negative bacteria. *New England Journal of Medicine*, *362*(19), 1804–1813. https://doi.org/10.1056/NEJMra0904124

Pereira de Sousa, I., & Bernkop-Schnurch, A. (2014). Pre-systemic metabolism of orally administered drugs and strategies to overcome it. *Journal of Controlled Release*, *192*, 301–309. https://doi.org/10.1016/j.jconrel.2014.08.004

Perez, C., Daniel, K. B., & Cohen, S. M. (2013). Evaluating prodrug strategies for esterase-triggered release of alcohols. *ChemMedChem*, *8*(10), 1662–1667. https://doi.org/10.1002/cmdc.201300255

Perinbam, K., & Siryaporn, A. (2018). A rapid image-based bacterial virulence assay using amoeba. *Journal of Visualized Experiments*, *136*. https://doi.org/10.3791/57844

Pitts, B., Hamilton, M. A., Zelver, N., & Stewart, P. S. (2003). A microtiter-plate screening method for biofilm disinfection and removal. *Journal of Microbiological Methods*, *54*(2), 269–276. https://doi.org/10.1016/S0167-7012(03)00034-4

Rautio, J., Kumpulainen, H., Heimbach, T., Oliyai, R., Oh, D., Järvinen, T., & Savolainen, J. (2008). Prodrugs: Design and clinical applications. *Nature Reviews Drug Discovery*, *7*, 255–270. https://doi.org/10.1038/nrd2468

Rautio, J., Kumpulainen, H., Heimbach, T., Oliyai, R., Oh, D., Jarvinen, T., & Savolainen, J. (2008). Prodrugs: Design and clinical applications. *Nature Reviews Drug Discovery*, *7*(3), 255–270. https://doi.org/10.1038/nrd2468

Sakimura, T., Kajiyama, S., Adachi, S., Chiba, K., Yonekura, A., Tomita, M., … Osaki, M. (2015). Biofilm-forming *Staphylococcus epidermidis* expressing vancomycin resistance early after adhesion to a metal surface. *BioMed Research International*, *2015*, 943056.

Schwarzenbach, G. A., Anderegg, G., & Sallmann, R. (1952). Der Phenolatsauerstoff als Koordinationspartner. *Helvetica Chimica Acta*, *35*(6), 1785–1793. https://doi.org/10.1002/hlca.19520350602

Singh, N., & Narayan, S. (2011). Nitazoxanide : A broad spectrum antimicrobial. *Medical Journal Armed Forces India*, *67*(1), 67–68. https://doi.org/10.1016/S0377-1237(11)80020-1

Stabnis, R. W. (2010). *Handbook of biological stains*. Hoboken, NJ: John Wiley and Sons Inc.

Stewart, P. S. (2002). Mechanisms of antibiotic resistance in bacterial biofilms. *International Journal of Medical Microbiology*, *292*(2), 107–113. https://doi.org/10.1078/1438-4221-00196

Stewart, P. S. (2015). Antimicrobial tolerance in biofilms. *Microbiology Spectrum*, *3*, 3. https://doi.org/10.1128/microbiolspec.MB-0010-2014

Stoodley, P., Cargo, R., Rupp, C. J., Wilson, S., & Klapper, I. (2002). Biofilm material properties as related to shear-induced deformation and detachment phenomena. *Journal of Industrial Microbiology and Biotechnology*, *29*(6), 361–367. https://doi.org/10.1038/sj.jim.7000282

Suter, C. M. (1941). Relationships between the structure and the bactericidal properties of phenols. *Chemical Reviews*, *28*(2), 269–299. https://doi.org/10.1021/cr60090a004

Takenaka, S., Trivedi, H. M., Corbin, A., Pitts, B., & Stewart, P. S. (2008). Direct visualization of spatial and temporal patterns of antimicrobial action within model oral biofilms. *Applied and Environmental Microbiology*, *74*(6), 1869–1875. https://doi.org/10.1128/AEM.02218-07

Tarn, D., Xue, M., & Zink, J. I. (2013). pH-Responsive dual cargo delivery from mesoporous silica nanoparticles with a metal-latched nanogate. *Inorganic Chemistry*, *52*(4), 2044–2049. https://doi.org/10.1021/ic3024265

Tawakoli, P. N., Al-Ahmad, A., Hoth-Hannig, W., Hannig, M., & Hannig, C. (2013). Comparison of different live/dead stainings for detection and quantification of adherent microorganisms in the initial oral biofilm. *Clinical Oral Investigations*, *17*(3), 841–850. https://doi.org/10.1007/s00784-012-0792-3

Tchouaffi-Nana, F., Ballard, T. E., Cary, C. H., Macdonald, T. L., Sifri, C. D., & Hoffman, P. S. (2010). Nitazoxanide inhibits biofilm formation by *Staphylococcus epidermidis* by blocking accumulation on surfaces. *Antimicrobial Agents and Chemotherapy*, *54*(7), 2767–2774. https://doi.org/10.1128/AAC.00901-09

Ueda, Y., Matiskella, J. D., Golik, J., Connolly, T. P., Hudyma, T. W., Venkatesh, S., … Bronson, J. J. (2003). Phosphonooxymethyl prodrugs of the broad spectrum antifungal azole, ravuconazole: Synthesis and biological properties. *Bioorganic & Medicinal Chemistry Letters*, *13*(21), 3669–3672. https://doi.org/10.1016/j.bmcl.2003.08.029

Venkatesan, N., Perumal, G., & Doble, M. (2015). Bacterial resistance in biofilm-associated bacteria. *Future Microbiology*, *10*(11), 1743–1750. https://doi.org/10.2217/fmb.15.69

Vuotto, C., Moura, I., Barbanti, F., Donelli, G., & Spigaglia, P. (2016). Subinhibitory concentrations of metronidazole increase biofilm formation in *Clostridium difficile* strains. *Pathogens and Disease*, *74*(2).

Wakamatsu, R., Takenaka, S., Ohsumi, T., Terao, Y., Ohshima, H., & Okiji, T. (2014). Penetration kinetics of four mouthrinses into *Streptococcus mutans* biofilms analyzed by direct time-lapse visualization. *Clinical Oral Investigations*, *18*(2), 625–634. https://doi.org/10.1007/s00784-013-1002-7

Walsh, D. J., Livinghouse, T., Durling, G. M., Chase-Bayless, Y., Arnold, A. D., & Stewart, P. S. (2020). Sulfenate esters of simple phenols exhibit enhanced activity against biofilms. *ACS Omega*, *5*(11), 6010–6020. https://doi.org/10.1021/acsomega.9b04392

Walters, M. C. III, Roe, F., Bugnicourt, A., Franklin, M. J., & Stewart, P. S. (2003). Contributions of antibiotic penetration, oxygen limitation, and low metabolic activity to tolerance of *Pseudomonas aeruginosa* biofilms to ciprofloxacin and tobramycin. *Antimicrobial Agents and Chemotherapy*, *47*(1), 317–323. https://doi.org/10.1128/AAC.47.1.317-323.2003

Walther, R., Rautio, J., & Zelikin, A. N. (2017). Prodrugs in medicinal chemistry and enzyme prodrug therapies. *Advanced Drug Delivery Reviews*, *118*, 65–77.

Wilhelm, S., Gdynia, A., Tielen, P., Rosenau, F., & Jaeger, K.-E. (2007). The autotransporter esterase EstA of *Pseudomonas aeruginosa* is required for rhamnolipid production, cell motility, and biofilm formation. *Journal of Bacteriology*, *189*(18), 6695–6703. https://doi.org/10.1128/JB.00023-07

Wu, K.-M. (2009). A new classification of prodrugs: Regulatory perspectives. *Pharmaceuticals (Basel, Switzerland)*, *2*(3), 77–81. https://doi.org/10.3390/ph2030077

Xie, J. L., Singh-Babak, S. D., & Cowen, L. E. (2012). Minimum inhibitory concentration (MIC) assay for antifungal drugs. *Bio-Protocol*, *2*(20), e252. https://doi.org/10.21769/BioProtoc.252

Xing, F., Cheng, G., & Yi, K. (2006). Study on the antimicrobial activities of the capsaicin microcapsules. *Journal of Applied Polymer Science*, *102*(2), 1318–1321. https://doi.org/10.1002/app.23766

Yonezawa, H., Osaki, T., Hojo, F., & Kamiya, S. (2019). Effect of *Helicobacter pylori* biofilm formation on susceptibility to amoxicillin, metronidazole and clarithromycin. *Microbial Pathogenesis*, *132*, 100–108.

Zhao, T., & Chen, Q. (2016). 9 - Halogenated phenols and polybiguanides as antimicrobial textile finishes. In G. Sun (Ed.), *Antimicrobial textiles* (pp. 141–153). Cambridge, UK: Woodhead Publishing.

Zhou, Q., Xiao, Q., Zhang, Y., Wang, X., Xiao, Y., & Shi, D. (2019). Pig liver esterases PLE1 and PLE6: Heterologous expression, hydrolysis of common antibiotics and pharmacological consequences. *Scientific Reports*, *9*(1), 15564. https://doi.org/10.1038/s41598-019-51580-4

SUPPORTING INFORMATION

Additional supporting information may be found online in the Supporting Information section.

How to cite this article: Walsh DJ, Livinghouse T, Durling GM, et al. Novel phenolic antimicrobials enhanced activity of iminodiacetate prodrugs against biofilm and planktonic bacteria. *Chem Biol Drug Des*. 2021;97:134–147. https://doi.org/10.1111/cbdd.13768